Self-similar clustering of inertial particles in homogeneous turbulence

HIROSHI YOSHIMOTO AND SUSUMU GOTO

Department of Mechanical Engineering and Science, Kyoto University,
Yoshida-Honmachi, Sakyo, Kyoto, 606-8501, Japan

It is shown by direct numerical simulation that the preferential concentration of small heavy particles in homogeneous isotropic developed turbulence has a self-similar multi-scale nature when the particle relaxation time is within the inertial time scales of the turbulence. This is shown by the pair correlation function of the particle distribution extending over the entire inertial range, and the probability density function of the volumes of particle voids taking a power-law form. This self-similar multi-scale nature of particle clustering cannot be explained only by the centrifugal effect of the smallest-scale (i.e. the Kolmogorov scale) eddies, but also by the effect of co-existing self-similar multi-scale coherent eddies in the turbulence at high Reynolds numbers. This explanation implies that the preferential concentration of particles takes place even when the relaxation time of particles is much larger than the Kolmogorov time, provided it is smaller than the longest time scale of the turbulence, since even the largest-scale eddies bring about particle clustering.

1. Introduction

The behaviour of small heavy particles in turbulence is investigated. This problem is ubiquitous in various systems such as droplet growth in atmospheric turbulence (Vaillancourt & Yau 2000), planet formation due to dust condensation in nebula turbulence (Cuzzi *et al.* 2001), industrial applications using powder, and so on, and therefore it has been investigated extensively by many authors from various perspectives (Maxey 1987; Eaton & Fessler 1994; Kostinski & Shaw 2001; Balkovsky, Falkovich & Fouxon 2001; Bec 2003, 2005; Falkovich & Pumir 2004; Duncan *et al.* 2005; Chen, Goto & Vassilicos 2006; Cencini *et al.* 2006, and references therein). It is well known, from direct numerical simulations (see the seminal work by Squires & Eaton 1991, for example) and laboratory experiments (see for example Yang & Shy 2005), that heavy small inertial particles distribute inhomogeneously even in statistically homogeneous turbulence. This preferential concentration of inertial particles plays a crucial role, for example, in the growth of droplets in clouds because the concentration is likely to lead to the enhancement of their collision rate and consequently their rate of coagulation. This preferential concentration has been explained by the role of coherent vortical structures in homogeneous turbulence (Wang & Maxey 1993); that is, heavy particles tend to be swept out of intense eddies due to centrifugal effects, and accumulate along the outer peripheries of eddies. Recall that even in homogeneous turbulence there exist coherent tubular eddies with radius of (see e.g. Goto & Kida 2003, and figure 6(*b*) below).

However, as recently pointed out (Boffetta, De Lillo & Gamba 2004; Goto & Vassilicos 2006) for particle clustering in two-dimensional turbulence, we cannot

ignore the effect of the self-similar multi-scale nature of coherent eddies in developed turbulence on particle clustering. Consequently, particle clustering becomes statistically self-similar, and, in contrast to the conventional belief, the preferential concentration is not necessarily most significant when the Stokes number (defined by (2.2) below) is around 1, i.e. when the typical time scale τ_p of inertial particles is comparable with the time scale of the Kolmogorov-scale eddies. One purpose of the present article is to show that the above conclusion for developed two-dimensional turbulence is also valid for particle clustering in three-dimensional turbulence: the preferential concentration takes place even when the Stokes number is larger than 1 in high Reynolds number turbulence, and it has a self-similarity reflecting the self-similarity of coherent eddies.

2. Model of small heavy particle motion

It is not trivial to describe the interaction between a particle and its surrounding fluid even if we assume that the particle is a rigid sphere. We employ the simplest equation of motion for a small heavy particle (Maxey & Riley 1983),

$$\frac{\mathrm{d}}{\mathrm{d}t}\, \boldsymbol{v}_p(t) = \frac{1}{\tau_p}(\boldsymbol{u}(\boldsymbol{x}_p(t), t) - \boldsymbol{v}_p(t)) \tag{2.1}$$

where $\boldsymbol{x}_p(t)$ and $\boldsymbol{v}_p(t)$ respectively stand for the position and the velocity of a particle at time t, and $\boldsymbol{u}(\boldsymbol{x}, t)$ is the velocity field of the surrounding fluid at position $\boldsymbol{x}$. We investigate the case that $\boldsymbol{u}(\boldsymbol{x}, t)$ is statistically homogeneous isotropic stationary turbulence of an incompressible fluid. In the derivation of (2.1), we assume that (i) the radius a of a spheric particle is small so that the fluid motion around the particle can be approximated by the Stokes flow, (ii) a is much smaller than the Kolmogorov length of the surrounding turbulence, (iii) the mass density ρ' of the particle is much larger than the fluid density, (iv) gravity is ignored. Furthermore, we assume that inertial particles are sufficiently dilute for particle collisions and the feedback of particle motion to fluid motion to be neglected.

The parameter τ_p $(= 2\rho'a^2/(9\mu)$ where μ is the fluid viscosity) in (2.1) stems from the Stokes drag coefficient of a sphere, and expresses the relaxation time of the velocity difference $\boldsymbol{u} - \boldsymbol{v}_p$. When τ_p is much larger than the longest time scale, i.e. the integral time $\mathcal{T}$, of the turbulence, such inertial particles are so inert that their motion may become independent of the fluid motion. On the other hand, when τ_p is smaller than the shortest time scale, i.e. the Kolmogorov time τ_η, of the turbulence, particle velocity relaxes quickly to the fluid velocity. Hence, in both the large and small τ_p limits, the preferential concentration of particles cannot be observed. In developed turbulence (note that $\mathcal{T}/\tau_\eta \sim R_\lambda$, the Taylor-length Reynolds number), there exist many time scales continuously between τ_η and $\mathcal{T}$. Therefore, as will be seen in §4 in detail, particle clustering is always observed when $\tau_\eta \lesssim \tau_p \lesssim \mathcal{T}$, or equivalently when the normalized particle relaxation time

$$S_\eta = \tau_p/\tau_\eta \tag{2.2}$$

is between $O(1)$ and $O(\mathcal{T}/\tau_\eta)$. S_η is called the Stokes number.

3. Direct numerical simulation

The turbulent velocity field $\boldsymbol{u}(\boldsymbol{x}, t)$ is numerically simulated by solving the Navier–Stokes equation,

$$\left(\frac{\partial}{\partial t} + \boldsymbol{u} \cdot \nabla \right) \boldsymbol{u} = -\frac{1}{\rho}\, \nabla\, p + \nu\, \nabla^2\, \boldsymbol{u} + \boldsymbol{f} \tag{3.1}$$

	N^3	R_λ	$\mathscr{L}$	$\mathscr{T}$	η	τ_η
Run A	128^3	60.0 ± 1.6	1.61 ± 0.07	2.17 ± 0.10	$(2.64 \pm 0.04) \times 10^{-2}$	$(1.40 \pm 0.04) \times 10^{-1}$
Run B	512^3	188 ± 6	1.87 ± 0.09	2.38 ± 0.10	$(5.55 \pm 0.05) \times 10^{-3}$	$(4.89 \pm 0.10) \times 10^{-2}$

TABLE 1. Statistics of the simulated turbulence. R_λ, Taylor-length Reynolds number; $\mathscr{L}$ integral length; $\mathscr{T}$, integral time; η, Kolmogorov length; τ_η, Kolmogorov time.
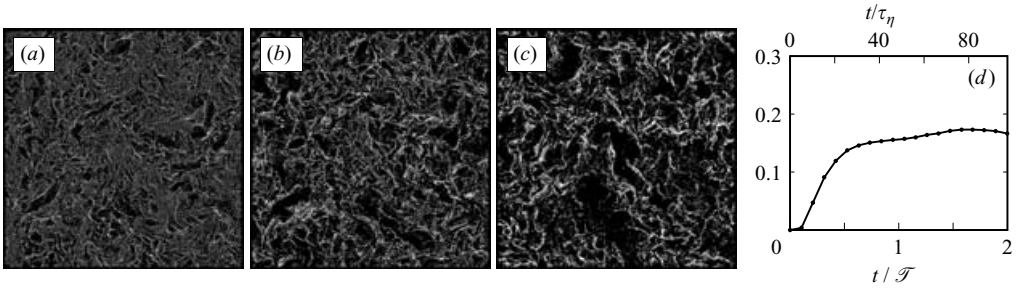

FIGURE 1. (*a–c*) Temporal evolution of inertial particles (white dots) of $S_\eta = 2$ inside a thin layer (side length $3.4\mathscr{L} \approx 1100\eta$, width 5η) at (*a*) $t \approx 5\tau_\eta \approx 0.11\mathscr{T}$, (*b*) $10\tau_\eta \approx 0.22\mathscr{T}$ and (*c*) $50\tau_\eta \approx 1.1\mathscr{T}$. Run B. A movie is available with the online version of the paper. (*d*) Temporal evolution of the total volume (normalized by the whole domain volume) of particle voids.

and the equation of continuity, $\nabla \cdot \boldsymbol{u} = 0$, of an incompressible fluid. Here, $p(\boldsymbol{x}, t)$, ρ and ν are the pressure field, constant density and kinematic viscosity, respectively. Periodic boundary conditions are imposed for three orthogonal directions, and we employ the Fourier spectral method to evaluate spatial derivatives. The fourth-order Runge–Kutta method is used for the time integration of (3.1). External forcing $\boldsymbol{f}$ is implemented by fixing the amplitudes of Fourier modes in a low-wavenumber region. Using 128^3 and 512^3 numerical grids we simulate turbulence at the Taylor-length Reynolds numbers $R_\lambda = 60.0$ and 188, respectively. Here, $R_\lambda = \sqrt{20/(3\nu\epsilon)}\,\mathscr{E}$, where $\mathscr{E}$ and ϵ are the energy per unit mass and its dissipation rate. Statistics of the simulated turbulence are listed in table 1, where $\mathscr{L} \equiv u'^3/\epsilon$ and $\mathscr{T} \equiv \mathscr{L}/u'$ (here $u' \equiv \sqrt{2\mathscr{E}/3}$ is the r.m.s. value of a velocity component) are respectively integral length and time, and $\eta \equiv \epsilon^{-1/4}\nu^{3/4}$ and $\tau_\eta \equiv \epsilon^{-1/2}\nu^{1/2}$ are respectively the Kolmogorov length and time.

The motions of inertial particles are simulated simultaneously with the fluid motion by solving (2.1) using the fourth-order Runge–Kutta method. We track $N_p = (N/2)^3$ particles in a simulation for figures 1(*a–c*), 2 and 3, and $N_p = N^3$ particles for figures 1(*d*), 5(*b*), 6 and 7. For figures 4, 5(*a*) and 9, we track up to $N_p = (6N)^3 \approx 4.5 \times 10^8$ particles in Run A to check the independence of particle cluster statistics of N_p. We simulated particles of eight different Stokes numbers ($S_\eta = 0.05, 0.1, 0.2, 0.5, 1, 2, 5$ and 10) for each Reynolds number. The initial positions of particles are distributed homogeneously.

4. Self-similar clustering of inertial particles
4.1. *Formation of clusters and voids of particles*

Figure 1(*a–c*) shows a temporal evolution of inertial particles of $S_\eta = 2$ in turbulence at $R_\lambda = 188$. The time elapsed in (*a*) to (*c*) is $5\tau_\eta \approx 0.11\mathscr{T}$, $10\tau_\eta \approx 0.22\mathscr{T}$ and $50\tau_\eta \approx 1.1\mathscr{T}$. Only the particles in a thin layer (width 5η, and side length $3.4\mathscr{L} \approx 1100\eta$) are plotted. After a duration of $O(\mathscr{T})$, inertial particles form clusters and empty regions
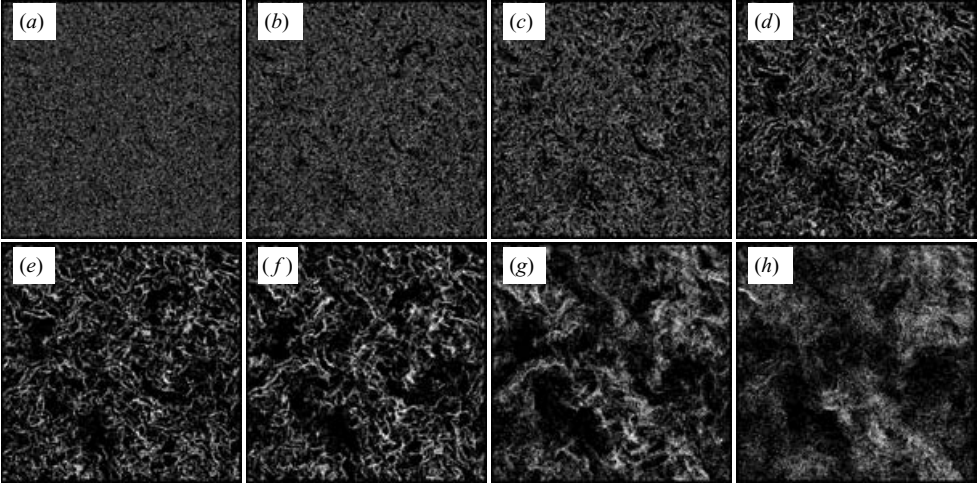
FIGURE 2. Spatial distribution of particles inside a thin layer (width 5η) for eight different Stokes numbers. The side length of plots is $3.4\mathscr{L} \approx 1100\eta$. $t \approx 2.1\mathscr{T} \approx 100\tau_\eta$. Run B. (a) $S_\eta = 0.05$, (b) 0.1, (c) 0.2, (d) 0.5, (e) 1, (f) 2, (g) 5 and (h) 10.

(voids). An important observation from these figures is that the clustering of particles is not well developed after only a few Kolmogorov times, but it saturates after the duration as long as the integral time $\mathscr{T}$. To show this quantitatively, we plot the temporal evolution of the total volume of voids of particles in figure 1(d). See §4.3 for the identification method of particle voids. It is clearly observed in this figure that it takes the long time of $O(\mathscr{T})$ for clustering statistics to saturate. This long saturation time implies that not only the smallest eddies but also larger ones play a role in the clustering of particles, which has been reported by Cencini *et al.* (2006) in terms of other quantities as well. It is also observed in figure 1(c) that the size of particle voids ranges between $O(\eta)$ and $O(\mathscr{L})$. This multi-scale nature of particle voids further implies the role of eddies larger than the Kolmogorov length.

The Stokes number dependence of particle clusters and voids is shown in figure 2, where the spatial distributions of particles in a thin layer (width 5η) for eight different S_η are visualized. We plot particle distributions after they become statistically stationary ($t = 2.1\mathscr{T}$). We can observe quite similar features to those of particle distributions in two-dimensional turbulence in the inverse energy cascade regime (Boffetta *et al.* 2004; Goto & Vassilicos 2006). When $S_\eta \lesssim 0.1$, the particle distribution is almost homogeneous and there are no clusters or voids (see figure 2a). When $S_\eta = O(0.1)$ there exist only small voids of size $O(\eta)$ (see figure 2b). As S_η increases, larger voids appear, but small voids of $O(\eta)$ still exist (see figure 2c–e). When $S_\eta = O(0.1\mathscr{T}/\tau_\eta)$, the size of the largest voids saturates at $O(\mathscr{L})$ (see figure 2f), and as S_η increases further, smaller voids become faint (see figure 2g, h).

These observations in figure 2 are qualitatively captured by the pair correlation function $m(\ell)$ of particle distribution. This function can be estimated by the formula (Kostinski & Shaw 2001; Landau & Lifshitz 1980)

$$\frac{1}{\ell} \int_0^\ell m(\ell')\, \mathrm{d}\ell' = \frac{\langle (\delta n)^2 \rangle_\ell}{\langle n \rangle_\ell^2} - \frac{1}{\langle n \rangle_\ell} \,. \tag{4.1}$$

Here, $\langle n \rangle_\ell$ and $\langle (\delta n)^2 \rangle_\ell$ are respectively the average and the variance of the number of particles inside boxes of size ℓ^3. Figure 3 shows $m(\ell)$, which is numerically estimated by
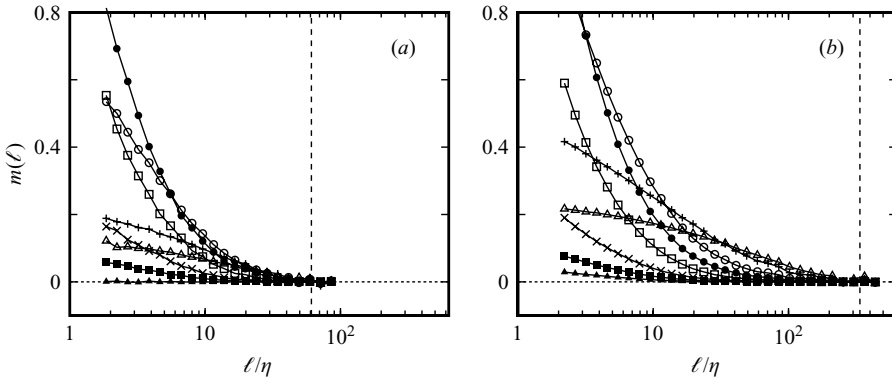
FIGURE 3. Pair correlation function. ▲, $S_\eta = 0.05$; ■, 0.1; ×, 0.2; □, 0.5; ●, 1; ○, 2. +, 5. △, 10. (*a*) Run A. $t \approx 1.8\mathcal{T}$. (*b*) Run B. $t \approx 2.1\mathcal{T}$. Vertical lines indicate $\ell = \mathcal{L}$.

differentiating the right-hand side of (4.1), for different Stokes numbers and Reynolds numbers. It is worth mentioning, in passing, that $m(\ell)$ is independent of the number N_p of particles for all $\ell(>\eta)$ if N_p is as large as the number N^3 of numerical grids. Figure 3 shows that (i) when S_η is smaller than 0.1, there is no clustering at any length scale larger than η, (ii) when S_η becomes slightly larger than 0.1, only the smallest-scale clustering takes place, (iii) as S_η continues to increase, larger clusters appear and the correlation extends over the integral length $\mathcal{L}$ (Notice that $m(\ell)$ extends over a wider range in Run B than A. It is confirmed (not shown, see Chen *et al.* (2006) for a similar result in the two-dimensional case) that $m(\ell)$ decays by a power law in the inertial length scales. Although the functional form in the viscous scales is not clear in the present simulation, it is consistent with the prediction by Balkovsky *et al.* 2001, i.e. a power law with an exponent different from the one in the inertial scales.), (iv) when S_η increases further, the pair correlation of smaller lengths starts decreasing to zero and (v) even when S_η is much larger than 1, large-scale correlations survive.

It must be emphasized that particles cluster even when S_η is much larger than 1. This is in contrast to the general belief that the concentration of particles is most significant when $S_\eta \approx 1$. The following subsections will bridge the gap between the conventional belief and the above observations of the Stokes number dependence and the multiplicity of void sizes.

4.2. *Physical picture of inertial particle clustering*

As shown by Goto & Vassilicos (2006) for the preferential concentration in two-dimensional turbulence, the Stokes number dependence of void sizes can be explained by the hypothesis that, depending on S_η, the size of eddies which play a role changes. Let $T(\ell) \sim \epsilon^{-1/3} \ell^{2/3}$ be the turnover time of eddies of size ℓ. Here, we choose the constant of proportionality for $T(\eta)$ to be τ_η. Then, the hypothesis states that eddies of size ℓ which satisfy a resonance condition

$$\alpha < \tau_p/T(\ell) < \beta \qquad (4.2)$$

centrifuge out inertial particles because particles promptly follow the slow fluid motion induced by large eddies with swirling time $T(\ell) \gg \tau_p$, while they completely ignore the fast fluid motion induced by small eddies with $T(\ell) \ll \tau_p$. Here, the non-dimensional parameters α and β are determined by the dynamics of the turbulence. A similar hypothesis based on the resonance between particles and eddies has been accepted by many authors (see the review by Eaton & Fessler 1994); however it was believed that

only the resonance of Kolmogorov-scale eddies played a role in particle clustering by homogeneous turbulence.

Since the figures 2 and 3 are quite similar to their counterparts in two-dimensional turbulence, it should be natural to apply the above hypothesis in terms of resonant eddies to the present three-dimensional case. Note that the two-dimensional turbulence treated in Goto & Vassilicos (2006) is similar to that considered here in the sense that the enstrophy spectrum in the inertial range is proportional to $k^{1/3}$ in the both cases.

The two parameters α and β in (4.2) may be estimated by considering the S_η dependence of $m(\ell)$. According to figure 3, irrespective of R_λ, $m(\ell)$ is negligibly small for all ℓ larger than η when S_η is smaller than 0.1. This implies that when $S_\eta \lesssim 0.1$ no eddy can contribute to the particle clustering. In other words, at $S_\eta \approx 0.1$ the smallest-scale eddies start playing a role; therefore we may roughly estimate $\alpha \approx 0.1$. On the other hand, at the length of the smallest eddies (5η, say) when S_η becomes greater than 2 the correlation function starts to decrease irrespective of the Reynolds number. This suggests that $\beta \approx 2$. These estimations of α and β are rough, but the following argument is robust for a small change of these values if their ratio β/α is not small but $O(10)$ and they are independent of R_λ.

The resonance condition (4.2) means that eddies, if any, which satisfy this condition, i.e. eddies of sizes between

$$\ell_{\min} = (S_\eta/\beta)^{3/2}\,\eta \qquad \text{and} \qquad \ell_{\max} = (S_\eta/\alpha)^{3/2}\,\eta, \qquad (4.3)$$

simultaneously contribute to particle clustering. As the inertial range is bounded by η and $\mathcal{L}$, the minimum length of resonant eddies is $\max\{\ell_{\min}, \eta\}$, whereas the maximum length is $\min\{\ell_{\max}, \mathcal{L}\}$. Therefore, in non-developed turbulence at small Reynolds numbers, the multi-scale nature of particle clustering is not significant; recall the relation $R_\lambda \sim (\mathcal{L}/\eta)^{2/3}$. This may be a reason why this nature was not apparent in the previous studies. The condition (4.2) also means that even if R_λ is infinitely large, the scale ratio $\ell_{\max}/\ell_{\min}$ of resonant eddies is bounded by $(\beta/\alpha)^{3/2} \approx 100$.

In summary, since multi-scale coherent eddies co-exist in developed turbulence, there are continuous length scales between $\ell_{\min}$ and $\ell_{\max}$. Consequently, clusters of inertial particles in turbulence at high Reynolds number also possess a multi-scale nature between these two lengths. This also explains, in terms of the role of eddies larger than η, why the preferential concentration of particles takes place even when S_η is much larger than 1.

4.3. Numerical verification of the picture

In order to quantitatively verify this multi-scale nature of particle clustering, we identify the voids of particles and estimate their volumes by extending the method suggested by Boffetta *et al.* (2004) for the two-dimensional case to its three-dimensional counterpart. First, we divide the whole domain into a set of small cubes of side length ℓ_b $(= 5\eta)$, and identify the cubes which do not contain any particles. Then, we check the connections between empty cubes, and estimate the size of voids by the total volume of connected empty cubes. Note that empty cubes are well-defined if the number N_p of particles is sufficiently large. This is qualitatively demonstrated in figure 4, where we plot inertial particles within a thin layer for four different N_p. It is observed that even if N_p increases, the number density of particles in clusters increases, and empty regions remain strictly empty. Quantitative arguments are given in the Appendix.

The probability density functions (PDF) of void volumes are plotted in figure 5 for different Reynolds numbers. The Stokes number S_η is chosen for the pair correlation
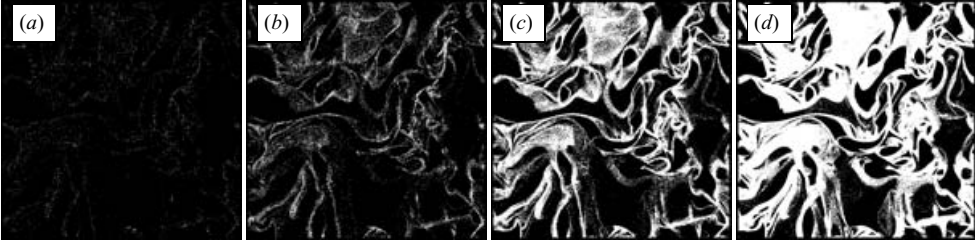
FIGURE 4. Spatial distribution of particles ($S_\eta = 1$) inside a thin layer (width 5η) for four different numbers N_p of particles. (a) $N_p = 64^3$, (b) 128^3, (c) 256^3 and (d) 512^3. Run A. Side length of plots is $3.9\mathscr{L} \approx 240\eta$.
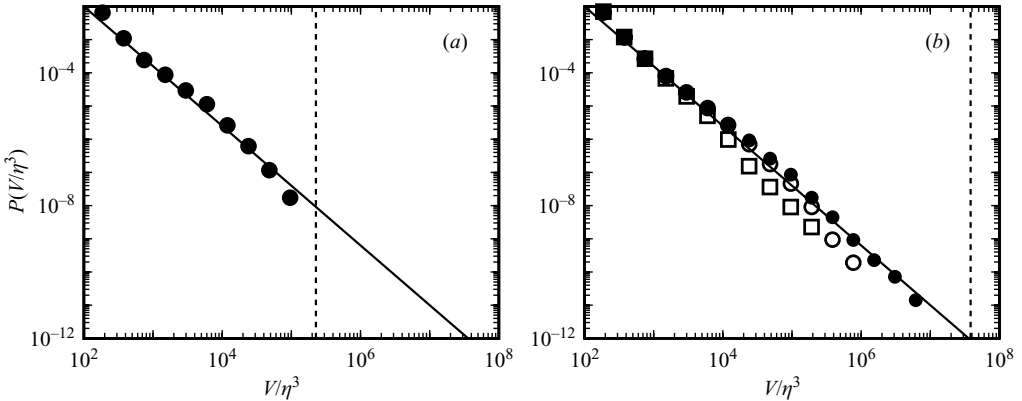

FIGURE 5. PDF of void volume of inertial particles. Solid lines indicate $V^{-1.8}$ power-law form, dotted vertical lines indicate $V = \mathscr{L}^3$. (a) Run A. $S_\eta = 1$. Average over 100 snapshots between $t = 1.8\mathscr{T}$ and $2.3\mathscr{T}$. (b) Run B. $S_\eta = 2$ (•), 0.5 (○) and 0.1 (□). Estimated by a snapshot at $t \approx 2.1\mathscr{T}$.

function $m(\ell)$ to be the broadest in ℓ; i.e. $S_\eta = 1$ for Run A and 2 for B. Two other S_η (0.1 and 0.5) cases are also plotted in figure 5(b) for comparison. We can see that larger voids exist in the larger Reynolds number flow, and that void volumes are distributed in a self-similar manner in the range $10^3\eta^3 \lesssim V \lesssim \mathscr{L}^3$ ($\approx 10^5\eta^3$ for Run A, and $10^7\eta^3$ for B), when S_η is appropriate for all eddies (from the smallest eddies of radius $O(10\eta)$ and length $O(10\eta)$ to the largest ones of radius $O(\mathscr{L})$ and length $O(\mathscr{L})$) to play a role. As evidence, a clear power law in the range, $10^3\eta^3 \lesssim V \lesssim \mathscr{L}^3$, is observed for such S_η. The exponent is about -1.8 irrespective of R_λ. Incidentally, if the volume of eddies of size ℓ is approximated by ℓ^3 (although this is a quite naive modelling of the coherent eddies in the present turbulence; see the next subsection) we can predict the exponent to be $-16/9$ by extending a model suggested by Goto & Vassilicos (2006) for two-dimensional turbulence to the present system.

It is also observed in figure 5(b) that as S_η increases the largest size of voids also increases. This is similar to two-dimensional turbulence (Boffetta *et al.* 2004) and consistent with the argument in the preceding subsection (i.e. ℓ_{max} is an increasing function of S_η).

It is this multiplicity, captured by the PDF (figure 5) of void volumes, that supports the hypothesis, suggested in the preceding subsection, of the formation of clusters and voids in turbulence. Multi-scale eddies satisfying (4.2) sweep out particles

simultaneously, and therefore the void volume PDF obeys a power law reflecting self-similarity of these eddies.

4.4. *Further consideration in terms of coherent eddies*

The smallest-scale coherent eddies are known to be thin tubes and their length varies between η and $\mathscr{L}$ although their radii are always the order of the Kolmogorov length η (see e.g. Goto & Kida 2003). This multiplicity might explain the power-law behaviour in the range of $O(\eta^3) < V < O(\eta^2\mathscr{L})$ of $P(V)$ for a small Stokes number ($S_\eta = 0.1$ in figure 5b), in which case only the Kolmogorov-scale eddies are resonant with the particles. (Incidentally, since the radius of the Kolmogorov-scale eddies is about 10η and their longest length is about $\mathscr{L} \approx 300\eta$ (see figure 7f below), the upper bound of the power-law range for $S_\eta = 0.1$ may be estimated as $10^5\eta^3$, which is consistent with figure 5b.) However, this multi-length nature of thin tubes cannot fully explain the multi-scale nature of voids observed in figure 5 for larger Stokes numbers. This is demonstrated in figure 6, where we visualize three (large, medium and small) voids for $S_\eta = 2$. The volumes of these voids are $(2.7 \times 10^6)\eta^3$, $(4.4 \times 10^5)\eta^3$ and $(6.4 \times 10^4)\eta^3$. In figure 6(b), the iso-surfaces of enstrophy are plotted together with these voids. The iso-surfaces look like thin vortex tubes, the radii of which are of the order of the Kolmogorov length. Although the size of the small void shown in figure 6 is comparable to the smallest-scale eddies, those of the large and medium voids are significantly different from the eddies. Therefore, it is not possible to explain the formation of all voids solely by the effects of the smallest-scale eddies.

In order to verify the picture suggested in §4.2 in terms of coherent eddies, we identify eddies of arbitrary size ℓ by iso-surfaces of coarse-grained squared vorticity $\omega_c(k_c)^2$ ($\equiv |\boldsymbol{\omega}_c(k_c)|^2$), which is obtained by the sharp low-pass filtering of Fourier modes of vorticity at cutoff wavenumber $k_c = 2\pi/\ell$. In figure 7(a), we plot the large void in figure 6 and the largest eddies (see figure 7b); k_c is chosen as 8, i.e. $\ell \approx 0.4\mathscr{L}$. The coincidence of the large void and one of the largest eddies is clearly observed. This implies that the formation of the largest-scale voids can be explained by the centrifugal effects of the largest-scale eddies. For the medium void in figure 6, the clear coincidence of the void and an intermediate-sized eddy can be confirmed in figure 7(c, d). Furthermore, it is also verified in figure 7(e, f) that the small void coincides with one of the smallest-scale eddies. These visualizations in figures 6 and 7 support the hypothesis that the multi-scale nature of void sizes (observed in figure 5) is due to the multi-scale nature of coherent eddies.

Note, in passing, that two kinds of self-similarities are likely to be embedded in the tubular vortical structures in this turbulence; one is in the longitudinal lengths of the vortex tubes (which is relevant to the power law of $P(V)$ for small S_η), whereas the other is in their radii (which is captured by the coarse-graining of the vorticity field). Therefore, the power-law behaviour of $P(V)$ for large S_η must reflect the overlap of these two self-similarities of coherent eddies.

To strengthen the qualitative verification developed above based on figures 6 and 7, we estimate the average coarse-grained squared vorticity (with cutoff wavenumber k_c) $\langle \omega_c(k_c)^2 | V \rangle_{\text{void}}$ at the position of particle voids of volumes between ξV and V (here $\xi = 0.5$). This conditional average is normalized by the spatial average $\langle \omega_c(k_c)^2 \rangle$, and plotted in figure 8(a). It is seen that this conditional average becomes maximum at a different cutoff wavenumber $\widetilde{k}_c(V)$ depending on V; more precisely, $\widetilde{k}_c(V)$ is a decreasing function of V as shown in figure 8(b). This supports the suggested hypothesis that larger voids are created due to centrifugal effects of larger eddies.
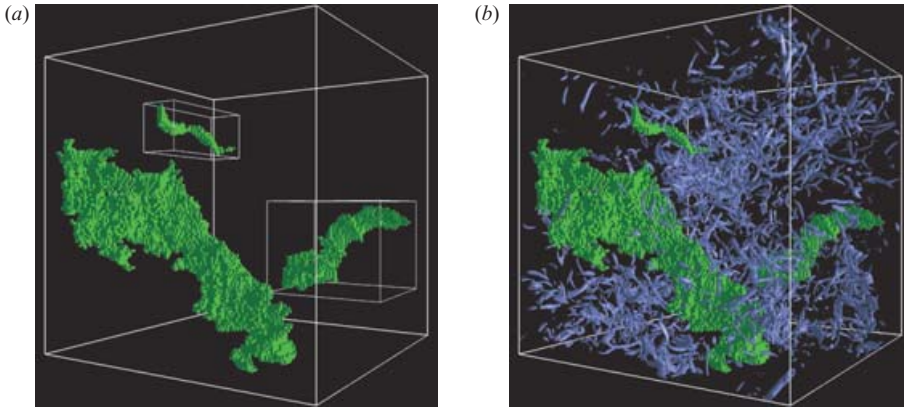
FIGURE 6. (*a*) Three typical voids of inertial particles of $S_\eta = 2$. Run B. The side length of box is $1.9\mathscr{L}(\approx 630\eta)$. Embedded boxes are magnified in figure 7. (*b*) Voids together with iso-surfaces of enstrophy (shown in blue). Threshold is chosen as the mean plus four standard deviations.
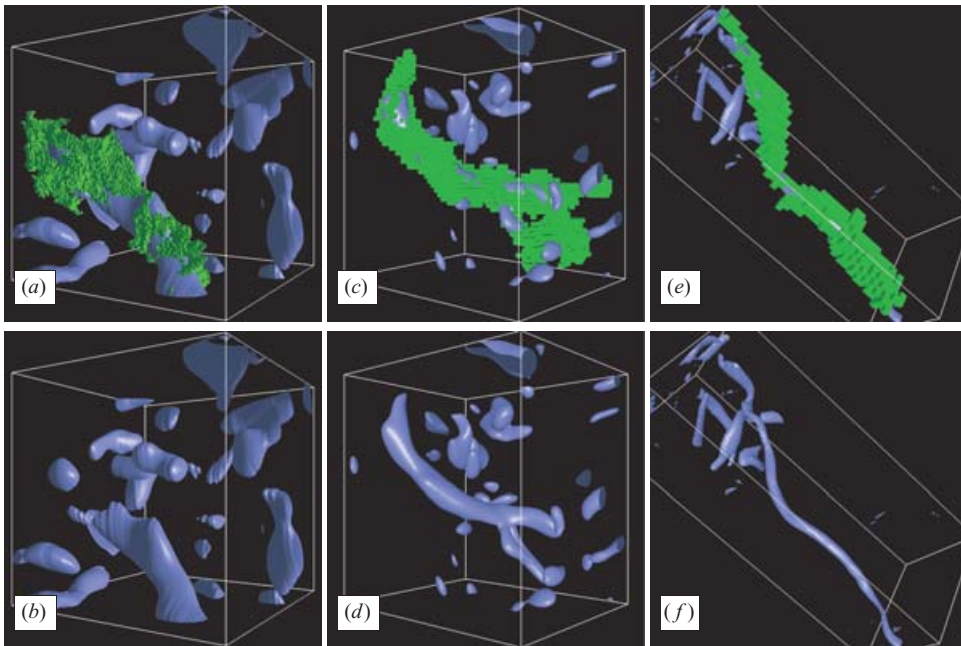

FIGURE 7. (*a*, *b*) The large void in figure 6 (green) and iso-surfaces of coarse-grained squared vorticity $\omega_c(8)^2$ (shown in blue). (*c*, *d*) The medium void in figure 6 and iso-surfaces of $\omega_c(32)^2$. The size of the plotted region is $0.76 \times 0.72 \times 0.60\mathscr{L}(\approx 260 \times 250 \times 200\eta)$. (*e*, *f*) The small void in figure 6 and iso-surfaces of enstrophy. The size of the plotted region is $0.75 \times 0.30 \times 0.24\mathscr{L}(\approx 250 \times 100 \times 80\eta)$. The thresholds of iso-surfaces are chosen as the mean plus (*a*, *b*) two or (*c–f*) three standard deviations.

5. Conclusion

The emphasis of the present article is on the hypothesis that not only the smallest-scale eddies but also larger ones can contribute to the preferential concentration of inertial particles in developed turbulence. More precisely, all resonant eddies which
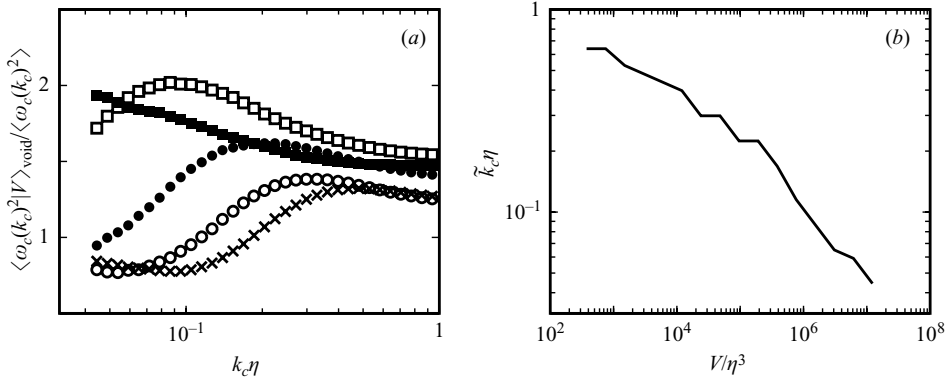
FIGURE 8. (*a*) Average coarse-grained squared vorticity (with sharp cutoff low-pass filtering at wavenumber k_c) at the position of particle voids with volumes between $0.5V$ and V. Normalized by the spatial average. $\times$, $V = (10\eta)^3$; $\circ$, $(20\eta)^3$; $\bullet$, $(40\eta)^3$; $\square$, $(80\eta)^3$; $\blacksquare$, $(160\eta)^3$. $S_\eta = 2$. Run B. (*b*) Wavenumber $\widetilde{k}_c(V)$ which gives the maximum value of the quantity plotted in (*a*).

satisfy (4.2) centrifuge out inertial particles simultaneously. One of the most important consequences of this hypothesis is that particles can cluster, due to the roles of eddies of larger scale than η, even when S_η is much larger than 1.

Our simulation at relatively high Reynolds numbers ($R_\lambda \approx 188$) supports this hypothesis and its consequences. Figure 1 shows that it takes longer than the turnover time of the largest eddies for particle clustering to reach a statistically stationary state. This is consistent with the fact that even the largest-scale eddies play a role in the clustering. Figures 2 and 3 support the statement that particle clustering takes place even when $S_\eta \gg 1$. It is also observed in figure 2 that the sizes of particle voids range between η and $\mathscr{L}$ when τ_p is within the inertial time scales of the turbulence. Furthermore, figures 5 and 7 show that the particle clustering in such cases becomes self-similar. This self-similar multi-scale nature of particle clustering can be explained as a reflection of the self-similar multi-scale nature of coherent eddies, which satisfy the resonance condition (4.2), in developed turbulence. (As a final part, note that it is well-known that a turbulent velocity field possesses a multifractal nature. Particle clustering is, therefore, also likely to be multifractal. This implies that particle clusters might not be self-similar in this strict sense, but the anomalous scaling brings only a small correction to the self-similarity considered in this article, which is mainly determined by low-order statistics of the velocity field. The multifractality of particle clustering is discussed in Bec (2005)).

Appendix. Dependence of $P(V)$ on N_p

In this Appendix, we consider the dependence of void volume statistics on the number N_p of particles. This dependence seems stronger than the void area statistics in two-dimensional turbulence, probably because voids are more easily connected in three-dimensional space. Nevertheless, we expect that the void volume statistics are well-defined if N_p is large enough, since even if we increase N_p, empty regions remain so (figure 4). To confirm this expectation, we plot in figure 9 the PDF $P(V)$ of void
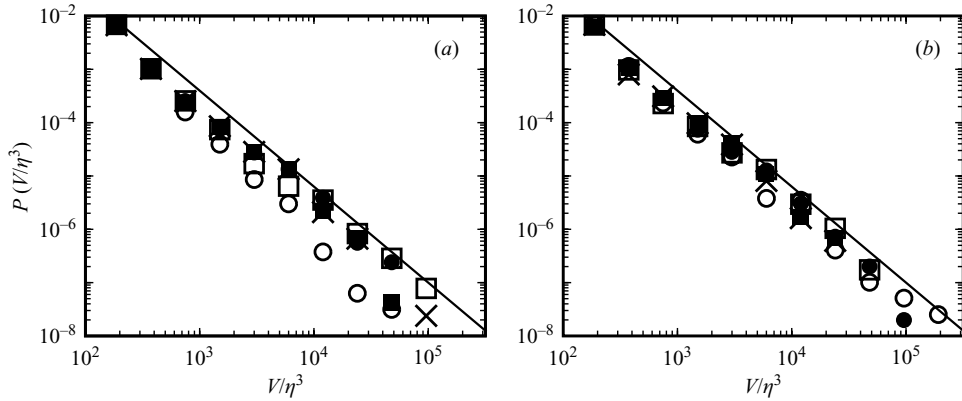
FIGURE 9. (*a*) The dependence of $P(V)$ on the number N_p of particles. $\circ$, $N_p = 64^3$; $\square$, 128^3; $\bullet$, 256^3; $\blacksquare$, 512^3; $\times$, 768^3. Run A. (*b*) PDF estimated for particles with virtual size $\ell_p = \eta$.

volumes for five different N_p for Run A (the numerical grids number is 128^3, and the grid width is about 1.9η). It is seen that when N_p is larger than 256^3, $P(V)$ is independent of N_p. This means that if we track at least $N_p = 256^3$ particles, i.e. eight times more than the number of numerical grids for Run A, in a simulation, we can capture well-defined void volume statistics. The PDF plotted in figure 5(*a*) is estimated using 512^3 particles.

However, it is numerically inefficient, or even impossible, to track such a huge number of particles for turbulence at larger Reynolds numbers. We suggest a numerical trick to estimate void volume statistics with a small number of particles. First, based on figure 4, we assume that particles exist only among other particles even if we increase N_p. Then, when we identify the empty cubes of size ℓ_b, and suppose that each particle virtually occupies a spherical volume of radius ℓ_p. Here, ℓ_p is chosen smaller than ℓ_b. It is confirmed, in figure 9(*b*), that $P(V)$ estimated thus is independent of N_p (for all N_p larger than 128^3 in Run A), and it is the same as $P(V)$, except for very large voids $V > 10^4\eta^3$, without this artificial procedure but with large $N_p (\geqslant 512^3)$. This result implies that this procedure indeed estimates $P(V)$ with a relatively small number of particles. In figure 5(*b*), we employ this trick to estimate PDF for Run B, where $N_p = 512^3$ and $\ell_p = \eta (= \ell_b/5)$ are used.

REFERENCES

BALKOVSKY, E., FALKOVICH, G. & FOUXON, A. 2001 Intermittent distribution of inertial particles in turbulent flows. *Phys. Rev. Lett.* **86**, 2790–2793.

BEC, J. 2003 Fractal clustering of inertial particles in random flows. *Phys. Fluids* **15**, L81–L84.

BEC, J. 2005 Multifractal concentration of inertial particles in smooth random flows. *J. Fluid Mech.* **528**, 255–277.

BOFFETTA, G., DE LILLO, F. & GAMBA, A. 2004 Large scale inhomogeneity of inertial particles in turbulent flow. *Phys. Fluids,* **16**, L20–L23.

CENCINI, M., BEC, J., BIFFERALE, L., BOFFETTA, G., CELANI, A., LANOTTE, A. S., MUSACCHIO, S. & TOSCHI, F. 2006 Dynamnics and statistics of heavy particles in turbulent flows. *J. Turbulence* **7**, 36.

CHEN, L., GOTO, S. & VASSILICOS, J. C. 2006 Turbulent clustering of stagnation points and inertial particles. *J. Fluid Mech.* **553**, 143–154.

CUZZI, J. N., HOGAN, R. C., PAQUE, J. M. & DOBROVOLSKIS, A. R. 2001 Size-selective concentration of chondrules and other small particles in protoplanetary nebula turbulence. *Astrophys. J.* **546**, 496–508.

DUNCAN, K., MEHLIG, B., ÖSTLUND, S. & WILKINSON, M. 2005 Clustering by mixing flows. *Phys. Rev. Lett.* **95**, 240602.

EATON, J. K. & FESSLER, J. R. 1994 Preferential concentration of particles by turbulence. *Intl J. Multiphase Flow* **20,** Suppl., 169–209.

FALKOVICH, G. & PUMIR, A. 2004 Intermittent distribution of heavy particles in a turbulent flow. *Phys. Fluids* **16**, L47–L50.

GOTO, S. & KIDA, S. 2003 Enhanced stretching of material lines by antiparallel vortex pairs in turbulence. *Fluid Dyn. Res.* **33**, 403–431.

GOTO, S. & VASSILICOS, J. C. 2006 Self-similar clustering of inertial particles and zero-acceleration points in fully developed two-dimensional turbulence. *Phys. Fluids* **18**, 115103.

KOSTINSKI, A. B. & SHAW, R. A. 2001 Scale-dependent droplet clustering in turbulent clouds. *J. Fluid Mech.* **434**, 389–398.

LANDAU, L. & LIFSHITZ, E. 1980 *Statistical Physics*. Pergamon.

MAXEY, M. 1987 The gravitational settling of aerosol particles in homogeneous turbulence and random flow field. *J. Fluid Mech.* **174**, 441–465.

MAXEY, M. & RILEY, J. 1983 Equation of motion of a small rigid sphere in a nonuniform flow. *Phys. Fluids* **26**, 883–889.

SQUIRES, K. D. & EATON, J. K. 1991 Preferential concentration of particles by turbulence. *Phys. Fluids* A **3**, 1169–1179.

VAILLANCOURT, P. A. & YAU, M. K. 2000 Review of particle-turbulence interactions and consequences for cloud physics. *Bull. Am. Met. Soc.* **81**, 285–298.

WANG, L. P. & MAXEY, M. R. 1993 Settling velocity and concentration distribution of heavy-particles in homogeneous isotropic turbulence. *J. Fluid Mech.* **256**, 27–68.

YANG, T. S. & SHY, S. S. 2005 Two-way interaction between solid particles and homogeneous air turbulence: particle settling rate and turbulence modification measurements. *J. Fluid Mech.* **526**, 171–216.